ORKUSTOFNUN

On non-1D effects in central-loop TEM-soundings for mapping of high-temperature geothermal systems

Knútur Árnason

Greinargerð KÁ-2001-01

ORKUSTOFNUN

Greinargerð
KÁ-2001/1

2001-02-7

ON NON-1D EFFECTS IN CENTRAL-LOOP TEM-SOUNDINGS FOR MAPPING OF HIGH-TEMPERATURE GEOTHERMAL SYSTEMS.

1. INTRODUCTION

Electrical methods have been used extensively for mapping high-temperature geothermal systems in Iceland. In the seventies and the eighties, DC-methods (mainly Schluberger soundings) were used, but since 1990, central-loop TEM-soundings have mainly be used. This is because the TEM-soundings turned out to be much more cost efficient and applicable under many conditions where the DC-methods could not be used.

2. Some general considerations

The interpretation of the apparent resistivity curves for the DC-soundings in terms of subsurface resistivity structure was first done by layered model curve fitting. In the seventies, one-dimensional (1D) layered earth inversion programs became available (eg. H.K. Johansen, 1972) and soon 1D-inversion became a routine. There were, however, frequently encountered sounding curves showing clear effects of non-layered resistivity structures which could not be fitted properly by layered models. An attempt was made to deal with this by simple qualitative interpretation based on catalogued response curves for simple models such as vertical or dipping plane resistivity boundaries.

In the late seventies, two-dimensional (2D) forward modelling codes for DC-resistivity methods became available (eg. Day and Morison, 1976) and 2D modelling gradually became common (in 2D models, resistivity can vary with depth and one lateral direction, but it is constant in the other perpendicular (strike) direction). With improved 2D forward algorithms and increasing computer power, 2D-inversion of DC-data became a common practice. In recent years 3D inversion of DC-data has even become attainable.

Forward calculations of responses for given resistivity models are in general much more complicated for controlled source electro-magnetic methods, like TEM, than for DC-methods. This implies that the interpretation software is much more complicated and computation intensive and only 1D-inversion is available for routine use at the moment. 2D-inversion is available for natural source, plain wave, Magneto-Tellurics (MT) and Controlled-Source-Magneto-Tellurics (CSMT) in the far field regime (plane wave approximation). The 2D approach is, however, not readily applicable for the controlled source TEM methods, because the source field is inherently three-dimensional (3D) and

any real progress from 1D inversion is full 3D modelling or full 3D-inversion.

There is no analytic solution to the general 2D and 3D problems, like for the layered 1D problem, and the forward problem has to be solved numerically which is a very computer intensive process. There exist, at present, several 3D forward codes for TEM, but only few of them are readily available and in general use. 3D forward modelling is therefore not a common practice yet. 3D-inversion is still on the research stage but some progress has been made recently.

When DC-methods were succeeded by central-loop TEM, there was, in a sense, taken a step backwards in the interpretation, from 2D inversion and to 1D-inversion. An important reason for using central-loop TEM in stead of DC-methods was, as stated earlier, that the TEM is much more cost-effective and can be applied in places where DC methods are not applicable. The question is, however, how much does the more simple interpretation of the TEM counteract these benefits.

There is no simple answer to this question and the answer will depend on how accurately the resistivity structure needs to be determined. If very detailed information is needed on shallow and lateral resistivity variations (from the surface and down to some tens of meters), then DC-methods with elaborate 2D or 3D inversion, are preferred and they are in fact used considerably in archaeological studies and studies of environmental impacts like toxic leakages.

If information on deeper resistivity structures is of primary concern, then some variants of electro-magnetic methods, including central-loop TEM, have inherently higher detect-ability than DC-methods. The reason is that increased depth of exploration can, for DC-methods, only be achieved by increasing the distance between the source and receiver locations (Árnason, 1984). This means that lateral variations of resistivity, at shallow and intermediate depths, have increasing influence on the measured response as the depth of exploration increases.

The depth of exploration in electro-magnetic methods can, like for DC-methods, be increased by increasing the source receiver separation. It can also be increased, with the source close to the receiver, by recording the response to later times (for TEM-methods) or lower frequencies (for frequency domain methods) and increasing the source moment, if necessary. The latter alternative leads to more downwards focused soundings which are less influenced by later variations at intermediate depths.

3. Intrinsic sensitivity of TEM soundings

The central-loop TEM method, with the receiver at the centre of the source loop, is probably one of the most downwards focused sounding methods. It can be shown theoretically (Nabighian, 1979), that in a homogeneous half-space, the induced currents of a source loop with constant current abruptly turned off, can be approximately though of as a diffuse current ring moving downwards and outwards from the source loop (like a blown "smoke ring"). The maximum of the current density in the smoke ring moves downwards and outwards from the source loop along a cone, making an about 30° angle with the surface, and at a speed proportional to the square-root of resistivity divided by

time.

It is to be expected that the sensitivity is high where the current density is high, and this is indeed the case. Figure 1 shows what might be called the "intrinsic sensitivity" for a central-loop TEM sounding, at different times after the current turn-off. A general 3D forward modelling code (Árnason, 1999) was used to calculate the transient response (dBz/dt) at the centre of 300mx300m square loop at the surface of a homogeneous half-space with resistivity 100Ωm (the centre of the loop is at x=0,y=0,z=0). The resistivity was then lowered from 100Ωm to 1Ωm in a cube of side length 100 m and the response calculated and compared to that of the homogeneous half-space. This was done for cubes at many different locations under the surface. Comparison of the perturbed and unperturbed responses gives information on the sensitivity to resistivity variations at different locations in the earth and how it changes with time after the source turn-off. The "intrinsic sensitivity" parameter is defined as:

$$s(x,y,z,t) = \log\left|\left(v_{pert}(x,y,z,t) - v_{ref}(t)\right)/v_{ref}(t)\right| \qquad (1)$$

where $v_{ref}(t)$ is the response of the homogeneous half-space at time t after the source turn-off and $v_{pert}(x,y,z,t)$ is the response when the resistivity is lowered from 100Ωm to 1Ωm in a cube of side length 100 m and centred at the point (x,y,z). s(x,y,z,t) defines a function of space and time which can be used to display the spatial distribution of the sensitivity and its evolution in time (the higher the value of s, the higher is the sensitivity).

Figure 1 shows the sensitivity in a vertical section through the sounding centre at the times of 0.11 ms, 0.33 ms, 1.1 ms, 3.3 ms, 11 ms, and 33 ms after the current turn-off. The figure clearly shows that at early times, the sensitivity is confined to shallow depths, and that it propagates do greater depths with increasing time. It is also seen that after about 1 ms, the sensitivity is highest on a cone dipping about 30° from horizontal, in accordance with the findings of Nabighian, as discussed above. It should be noted that the sensitivity decreases with depth at all times. One might have expected that a maximum would be observed, propagating downwards and outwards, along with the maximum of the current density and that, at late times, the response would become relatively insensitive to shallow resistivity structures (a misconception sometimes seen in the literature). This is not the case because current density at shallow depths, even though it is lower than at greater depths, produces stronger response because of its proximity to the receiver. A further important property is observed on figure 1, namely that, except at shallow depths, the central-loop TEM sounding is quite insensitive to the resistivity distribution right beneath the sounding centre.

A similar study of the intrinsic sensitivity of TEM methods, where the source and receiver are moved away from each other (Árnason, et.al., 2000a) shows that the sensitivity is highest in-between the source and the receiver, and at all times decreasing with depth. This implies that when the depth of exploration is increased by increasing the source receiver-distance, then lateral resistivity variations play an increasing role and 1D inversion may fail to give realistic results.

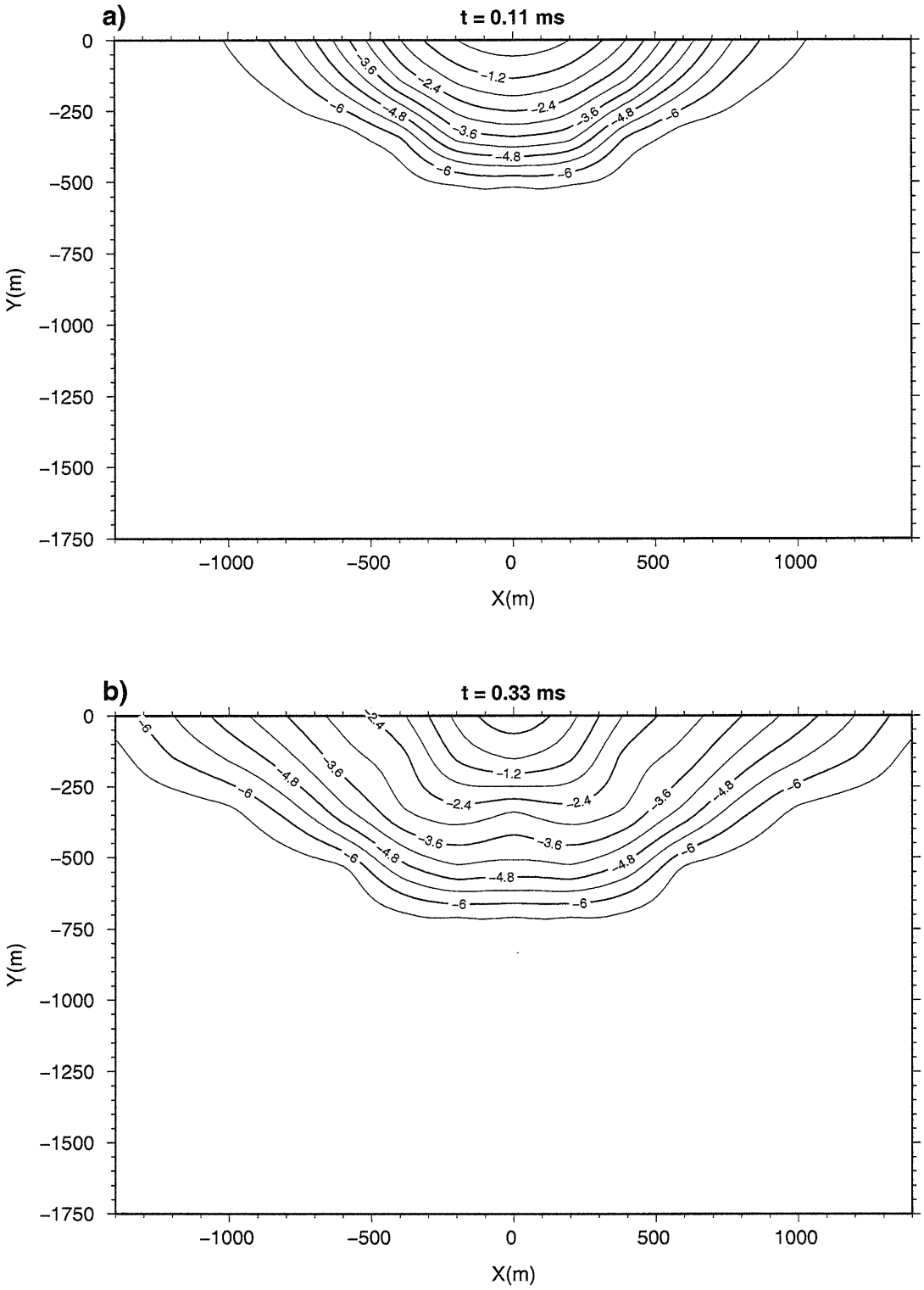

Figure-1. Intrinsic sensitvity of cuntral-loop TEM (vertical section) at 0.11 ms (a) and 0.33 ms (b) after source current turn off.

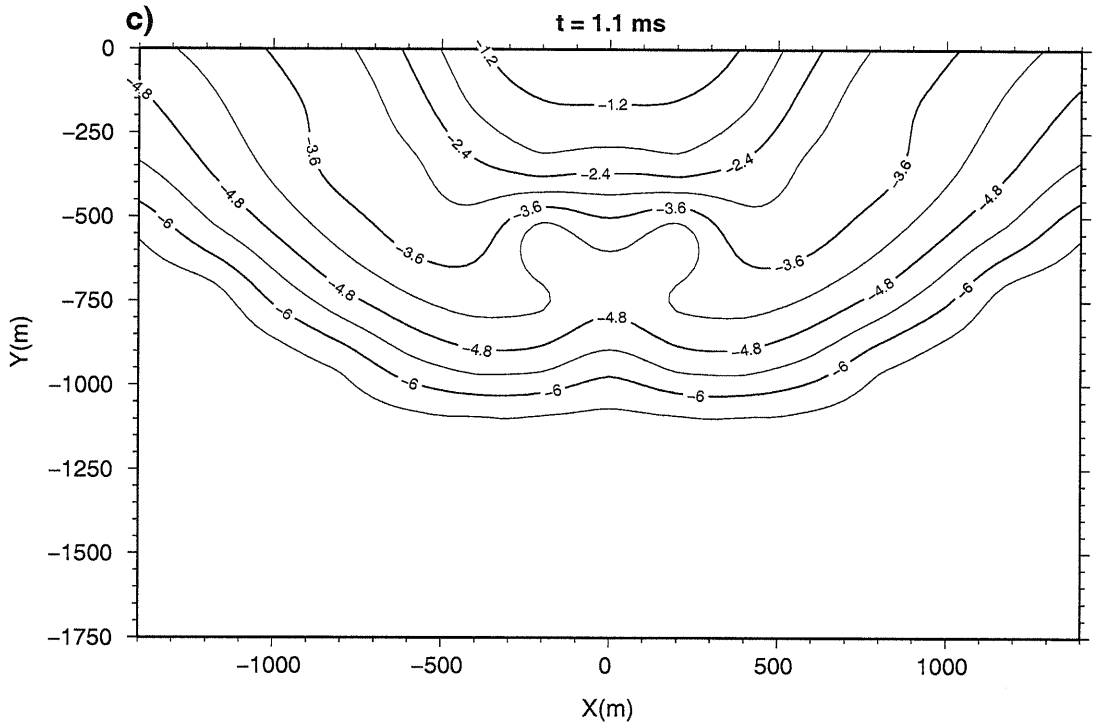

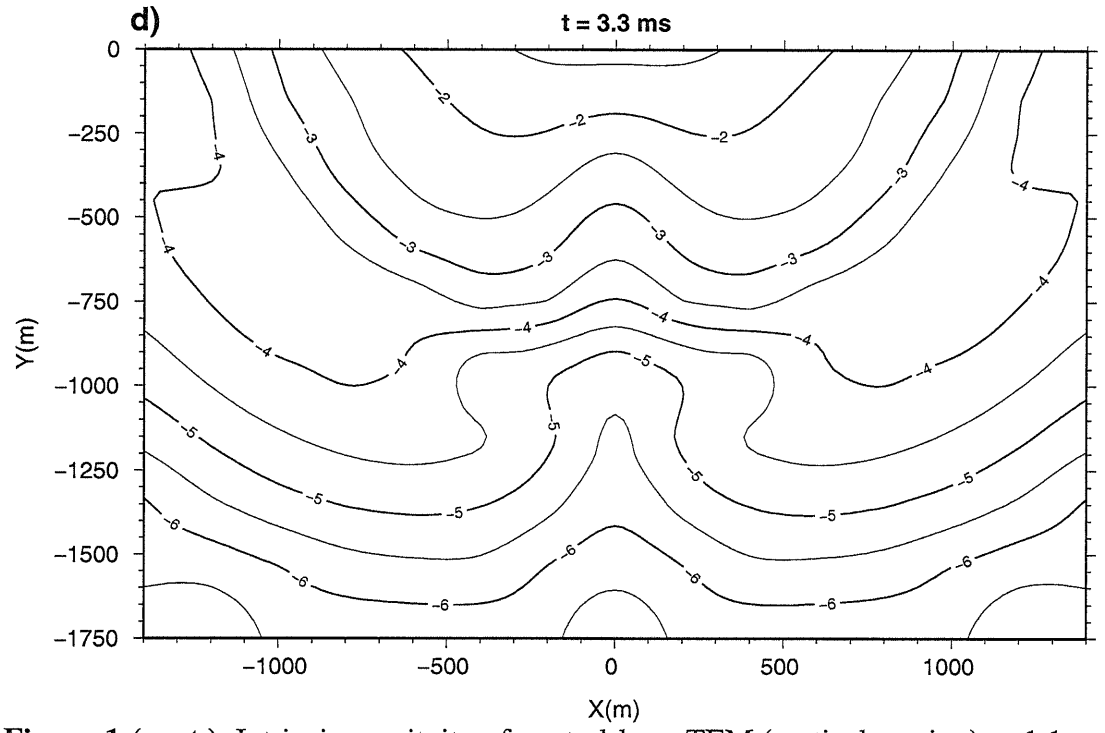

Figure-1 (cont.). Intrinsic sensitvity of cuntral-loop TEM (vertical section) at 1.1 ms (c) and 3.3 ms (d) after source current turn off.

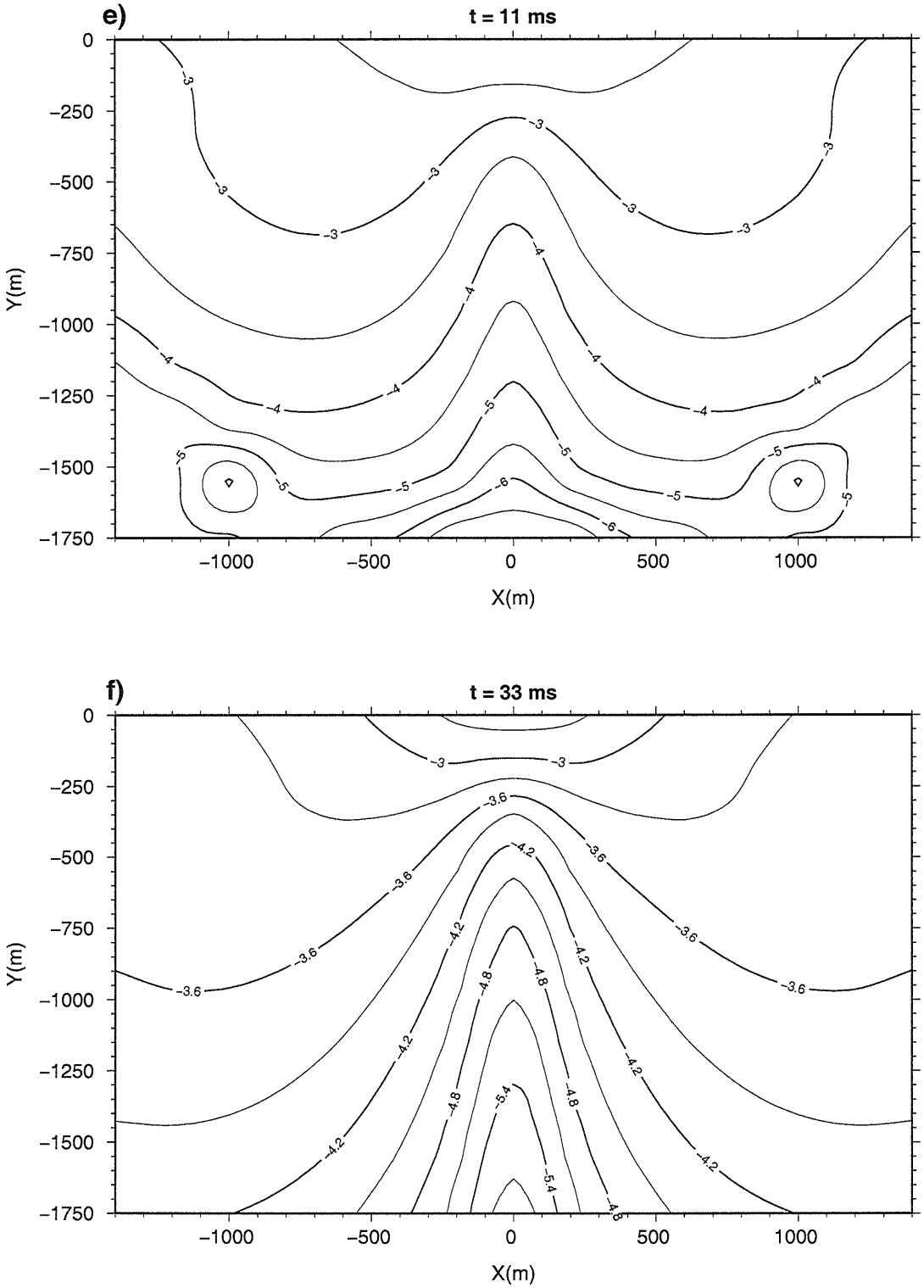

Figure-1 (cont.). Intrinsic sensitvity of cuntral-loop TEM (vertical section) at 11 ms (e) and 0.33 ms (f) after source current turn off.

The central-loop TEM configuration has one important property which is worth recognising. Since the source is a horizontal current loop, the induced currents in the ground are predominantly horizontal and are in fact strictly horizontal if the resistivity is horizontally stratified. The receiver is likewise a horizontal coil, which only couples to horizontal components of current density (the vertical component of the current density does not contribute to the vertical component of the magnetic field). Therefore the central-loop TEM sounding is more sensitive to vertical resistivity variations and suppresses effects of lateral (horizontal) variations.

In the case of DC-soundings, such as Schlumberger soundings, current is induced by sources at the surface. Currents penetrating to depth are bound to have predominant vertical component in the vicinity of the sources. As a result, the central-loop TEM soundings have much better vertical resolution than DC-methods (Árnason, 1995). The inevitable vertical components of the current density in the DC-methods makes them more sensitive to lateral resistivity variations than central-loop TEM. A comparison of 2D modelling of DC-data and 1D-inversion of TEM soundings, along the same profile in nearly 2D environment with sharp lateral variations, has shown that the 1D inversion of the TEM data gives only a little more smeared out results than the 2D modelling of the DC data (Árnason et.al., 1987).

The conclusion is that even though switching from DC-methods to TEM soundings means a step backwards in the dimensionality of the routine interpretation procedure, from 2D- to 1D-inversion, the loss in resolution is, in most cases, outweighed by the much higher cost efficiency.

Even though central-loop TEM is more downwards focused than other sounding methods and with 1D-inversion working rather well, it must always be kept in mind that lateral resistivity variations can, and often do, influence the response considerably. This should be evident by observing the wide spread intrinsic sensitivity displayed in figure 1. In extreme cases, sounding curves are obtained which can not be fitted properly by layered models. The most tricky situation is, however, when lateral variations disturb the sounding curves moderately and in such a way that they can still be fitted satisfactorily by 1D models which do not give a honest information about the resistivity structure underneath the sounding. Special care must be exercised when interpreting resistivity maps and sections obtained by 1D-inversion in terms of geothermal parameters, in areas where the resistivity structure is highly 3D.

4. Geothermal interpretation of resistivity structure

All high-temperature geothermal systems within the basaltic crust in Iceland show similar resistivity structure (Árnason et.al., 2000b). It is characterised by a low-resistivity cap ($\leq$10 Ωm) at the outer margins of the reservoir which is under-lain by about an order of magnitude more resistive core in the inner part. This is found in fresh-water systems as well as brine systems, with the same character but lower resistivities in the brine systems.

Comparison of this resistivity structure with data from wells has shown a good correlation with alteration mineralogy. The high conductivity in the low-resistivity cap is

thought to be due to conductive clay minerals in the so-called smectite-zeolite zone in the temperature range of 100-220°C. In the temperatures 220-240°C the conductive smectite is gradually replaced by the resistive chlorite mineral. At temperatures exceeding 250°C, chlorite and epidote are the dominant minerals and the resistivity is probably dominated by the pore fluid conduction in the high-resistivity core. The important consequence of this is that the resistivity structure can be interpreted in terms of temperature distribution, provided that the dominant alteration mineralogy is in equilibrium with temperature.

The above described correlation between resistivity and alteration mineralogy is based on comparison of resistivity structure obtained from 2D modelling of DC data and 1D-inversion of TEM data and analysis of alteration minerals in wells from several high-temperature geothermal areas in Iceland. This has gradually become a "standard model" for interpreting results of resistivity surveys in terms of alteration mineralogy and temperature distribution (assuming equilibrium between alteration and temperature).

5. Some 2D/3D effects in TEM soundings

The success of using the standard model to predict temperature distribution and for selecting promising drilling targets is ultimately depending on the reliability of the underlying resistivity model. The reliability of the resistivity structure obtained by a resistivity survey must always be a matter of concern. Systematic errors and artifacts, either in the sounding data or from the interpretation, can lead to wrong decisions and waste of money.

In the case of large and relatively homogeneous geothermal systems and not with to sharp boundaries, 1D-inversion of TEM soundings will almost certainly revile the true resistivity structure quite well. The situation can be quite different for geothermal systems with limited lateral extensions and/or complex internal structure and sharp boundaries. In this case 3D effects can lead to artifacts in 1D inversion, which can be erroneously interpreted in terms of alteration mineralogy. This can only be safely avoided by full 3D modelling or inversion, which is not within practical reach yet.

Relatively simple model calculations can, however, be used to gain insight into the problem and help to develop some feeling for where care must be taken when interpreting the resistivity structure. As the first attempt to do so, a 3D forward modelling code (temddd; Árnason, 1999) was used to calculate central-loop TEM apparent resistivity curves for some simple models. The models were fitted into a finite difference grid with 300 m grid spacings at the central part of the model and progressively increasing towards the edges. Calculated central-loop TEM apparent resistivity curves for 300mx300m source loops were then interpreted by 1D-inversion in order to investigate the effects of lateral variations in resistivity.

Four models are presented here. The first two have 2D resistivity structure, a dipping 2D boundary and a 2D low-resistivity ridge. The second two models have a 3D conical low-resistivity anomaly, meant as simple representation of a small geothermal system. In one of the models the interior of the cone has a homogeneous low resistivity, but in the other model the cone has a core of higher resistivity, according to the standard model. In all the

models, the boundaries between low resistivity and the more resistive hosts dip by 45°. This is probably, in many cases, an exaggeration of the real situation. The hydrology of high-temperature geothermal systems is, however, driven by convection and often strongly influenced by near vertical structures of tectonic or volcanic origin and sharp and steeply dipping boundaries are quite common.

5.1 2D dipping contact

This model consists of a 2D dipping contact along a strike. Figure 2 shows a vertical section through the model, perpendicular to the contact strike (resistivity does not change perpendicular to the section). The model has high resistivity surface layer of 1000 Ωm (dark blue), 150 m thick above the low-resistivity area to the left and 300 m thick over the higher resistivity part to the right. From left to right a low-resistivity region of 10 Ωm (light red) dips, down by 45° from 150 m depth and down to 3.6 km depth, contacting a homogeneous layer of 100 Ωm (light blue) to the right.

Seventeen central-loop TEM sounding curves were calculated, at 600 m intervals along a profile perpendicular to the dipping contact (numbered from 1 to 17, see figure 2). A resistivity section compiled from the layered models from 1D-inversion of the sounding curves is shown on figure 3 (the calculated sounding curves and their interpretation are shown in appendix A).

For soundings to the left of the contact, the interpretation gives thin layers with variable resistivity and total thickness of about 200 m, close to surface. The variable resistivity values are an artifact of limited accuracy of the calculated apparent resistivity curves at early times, due to the coarse gridding and big resistivity contrast, 1:100, (it is inherent property of the finite-difference method that fine grids are needed close to the surface in order to attain good accuracy at early times).

Soundings further than 1.5 km to the left of the dipping contact (soundings 1 through 7) give practically the true resistivity of the model at depth. Closer to the contact, the soundings start to see the higher resistivity to the right and the 1D-inversion gives progressively higher resistivity at depth, with the highest value of 15 Ωm at sounding nr. 9, just to the left of the surface extension of the contact. For soundings to the right of the top of the dipping contact, the interpreted basement resistivity decreases again with distance from the contact. Close to, and to the right of the base of the dipping contact (soundings 14 to 17), the basement resistivity is lower than the true resistivity of the model, because this time the soundings are affected by the low-resistivity to the left of the contact. Still further on the resistive side of the contact, the basement resistivity is bound to approach the true resistivity again.

In the resistive (100 Ωm) region to the right of the contact, the 1D-inversion gives more complex structure with values lower than the true value. Closest to the contact, there is a layer with resistivity values in the range of 19–25 Ωm which thickens from left to right. The lower boundary of this layer coincides surprisingly well with the true contact so the 1D-inversion reflects the dipping contact quite well even though the resistivity contrast is lower. This is a very important and encouraging observation. One might suspect that this is because the contact is a 45° dipping 2D model contact, but, as will be seen later, this is also the case for 3D models.

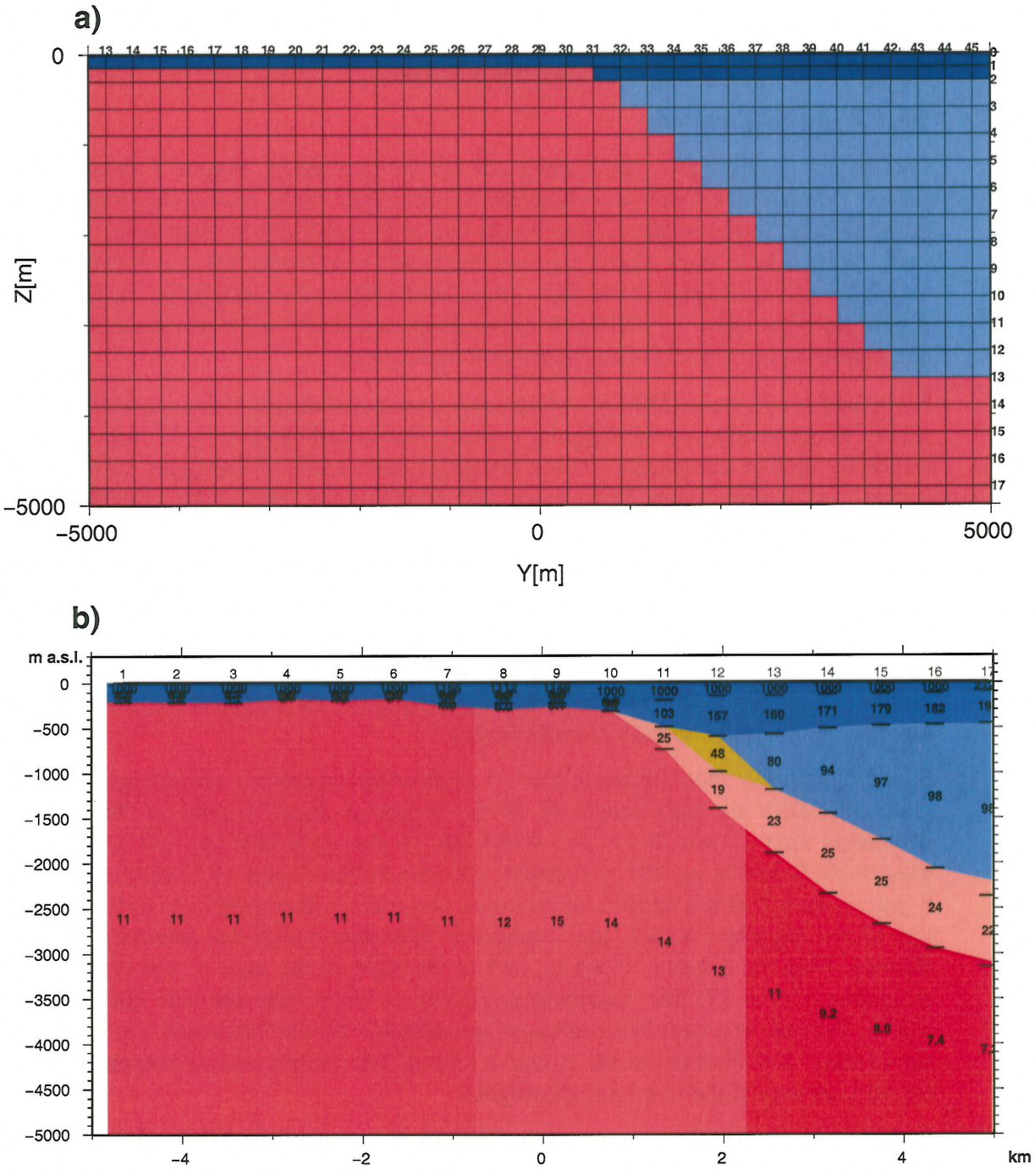

Figure-2. a), 45° dipping resistivity contrast between 10 Ωm (red) and 100 Ωm (blue), with 1000 Ωm surface layer (dark blue). b) a resistivity section based on 1D-inversion of synthetic central-loop sounding data.

A 100-150 m thick layer of 1000 Ωm is at the surface and below that is a 300-500 m thick layer with resistivity increasing from about 100 to 200 Ωm. Between these layers and the layer above the contact is a wedge shaped layer with resistivity increasing from about 50 Ωm, closest to eh contact and up to about the true value of 100 Ωm at sounding 17, about 1 km to the right of the base of the dipping contact.

The most important lessons learned from this model are that the dipping boundary is fairly well delineated by the top of the basement. The resistivity at depth, obtained from 1D-inversion for soundings close to the surface extension of the contact, is somewhat higher (up to about 50% for this model) than the true value. The effects of a dipping 2D contact do, however, not seem to lead to fictitious higher resistivity below low-resistivity (the shallow low-resistivity layers to the left of the contact are probably artifacts of limited accuracy, at early times, in the calculated curves). Figure 3 shows that the lowering on the high resistivity side is more pronounced than the increase on the low-resistivity side, reflecting the fact that the TEM method is more sensitive to low resistivity than high resistivity.

5.2 2D-low-resistivity ridge

This model consists of infinitely long low-resistivity ridge of 10 Ωm on a 10 Ωm basin. Figure 4 shows a vertical section, perpendicular to the ridge. The ridge has a 3.9 km plateau on the crest and dips by 45° on both sides, down to the basement at 3.6 km depth. The ridge is bordered by 100 Ωm to the sides and there is a 1000 Ωm surface layer, 150 m thick over the top of the ridge and 300 m thick to the sides.

Apparent resistivity curves were calculated for 300mx300m central-loop TEM soundings at 600 m intervals on a profile perpendicular to the ridge, from the the centre and out to 6 km distance. The sounding curves were then interpreted by 1D-inversion and the layered models used to compile the resistivity section shown on figure 5 (the synthetic curves and their 1D interpretation are shown in appendix B). The figure does actually show a symmetric 24 km long profile across the ridge. Figure 5 shows, as was to be expected, very similar resistivity structure to the sides of the ridge, as for the resistive side of the dipping contact on figure 3. The 100 Ωm region of the model appears as layers with intermediate resistivity but the slopes of the ridge are fairly well mapped by the top of low-resistivity basement, which again shows values lower than 10 Ωm at the ends of the profile, due to low resistivity to the side.

Under the plateau of the ridge, a low-resistivity layer is observed which approximately reflects the true resistivity of the region. The layer is relatively thick at the centre and gets progressively thinner towards the edges of the ridge, but the important finding is that, due to the higher resistivity to the sides, the low-resistivity layer appears as underlain by a fictitious higher resistivity. The region under the slopes does not show higher resistivity below low-resistivity but has values somewhat higher than the true resistivity value of the model.

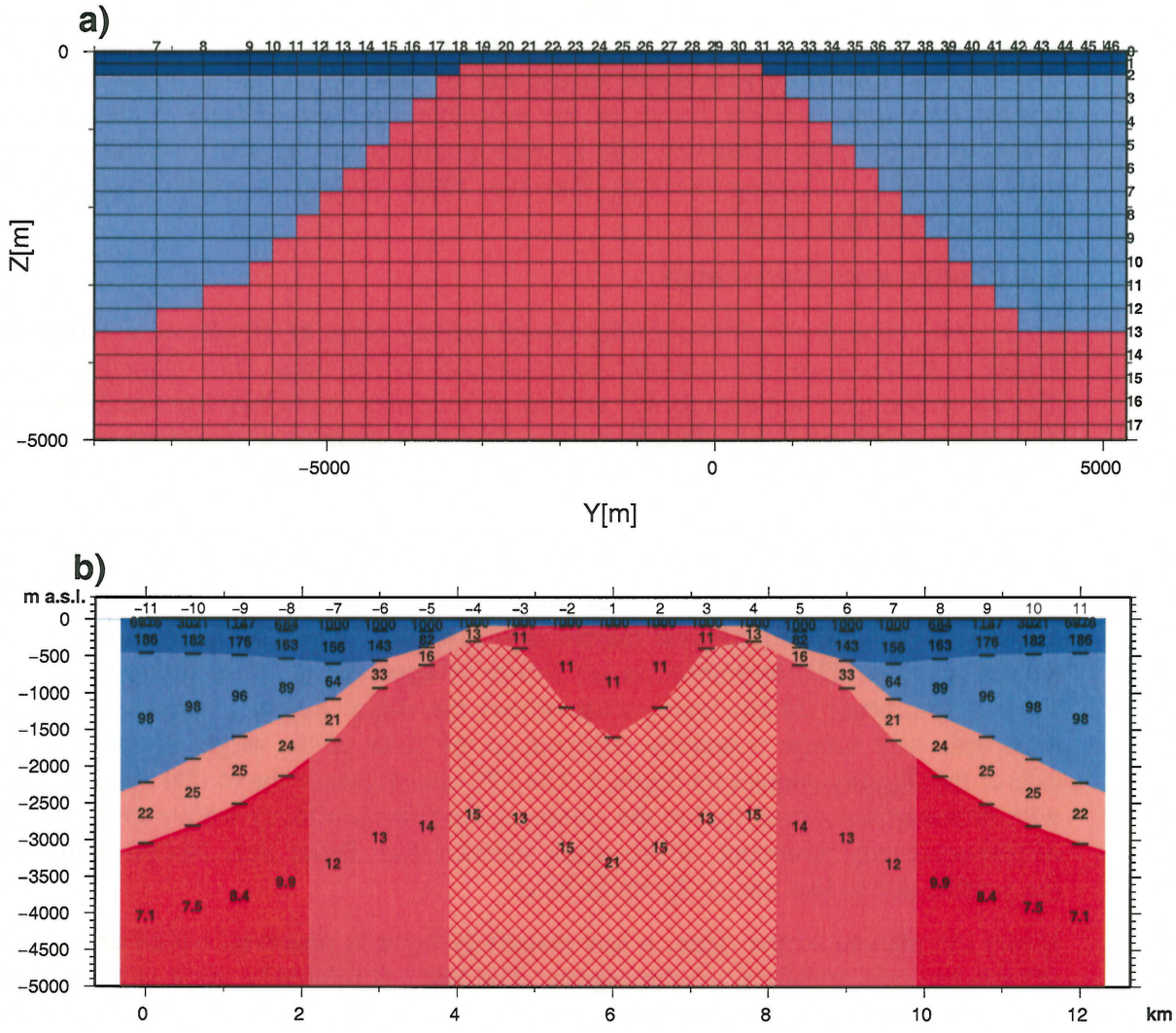

Figure-3. a), 2D 10 Ωm ridge (red), dipping 45° bordered by 100 Ωm (blue), and a 1000 Ωm surface layer (dark blue). b) a resistivity section based on 1D-inversion of synthetic central-loop sounding data.

Figure 5 clearly demonstrates that lateral resistivity variations can lead to fictitious higher resistivity below low-resistivity. The actual values of the higher resistivity are relatively moderate for this model, but the contrast would probably increase with higher contrast in the model. For a narrower ridge, one would expect a thinner low-resistivity layer and probably somewhat higher values below.

5.3 3D low-resistivity cone

The next model is designed to study effects of lateral resistivity variations in the case of a small hypothetical geothermal system, and is shown in a vertical section on figure 6. The model is a low-resistivity cone of 10 Ωm (light red). The cone has a diameter of 1.8 km at 150 m depth and with the sides dipping by 45° down to the depth of 3.6 km, where it sits on a 10 Ωm basement. The cone is surrounded by 100 Ωm (light blue) and a 1000 Ωm surface layer (dark blue), 150 m thick on top of the cone and 300 m thick out side it.

As before, the 3D code was used to calculate central-loop TEM sounding curves (300mx300m source loop) on profile across the cone and layered models from 1D-inversion were used to compile a resistivity section under the profile, as shown on figure 7 (the synthetic data and their interpretation are shown in appendix C).

Figure 7 shows that outside the cone the high resistivity is fairly well resolved to the depth of 1000-1500 m. Below is a rather thick layer of intermediate resistivity (40–55 Ωm) and under-lain by low-resistivity which approaches the true basement resistivity towards the end of the section. The upper boundary of this low resistivity reflects the boundary of the cone fairly well at the foot of the cone, but at the middle of the slope, a rather thick layer of about 30 Ωm is extending well down into the cone and is under-lain by higher resistivity. Closer to the centre of the cone a near surface low-resistivity layer is observed which reflects the boundary of the cone relatively well. At the top of the cone, the resistivity of the low-resistivity layer is close to the true value. Below the low-resistivity layer, there appears a considerably higher resistivity, even up to the order of thousand Ωm at the centre. This clearly demonstrates that lateral resistivity variations can lead to a fictitious resistive core in 1D-inversion. The resistivity values below the low-resistivity are, as was to be expected, much higher in the 3D case than in the 2D case above because the cone is surrounded by higher resistivity in all directions.

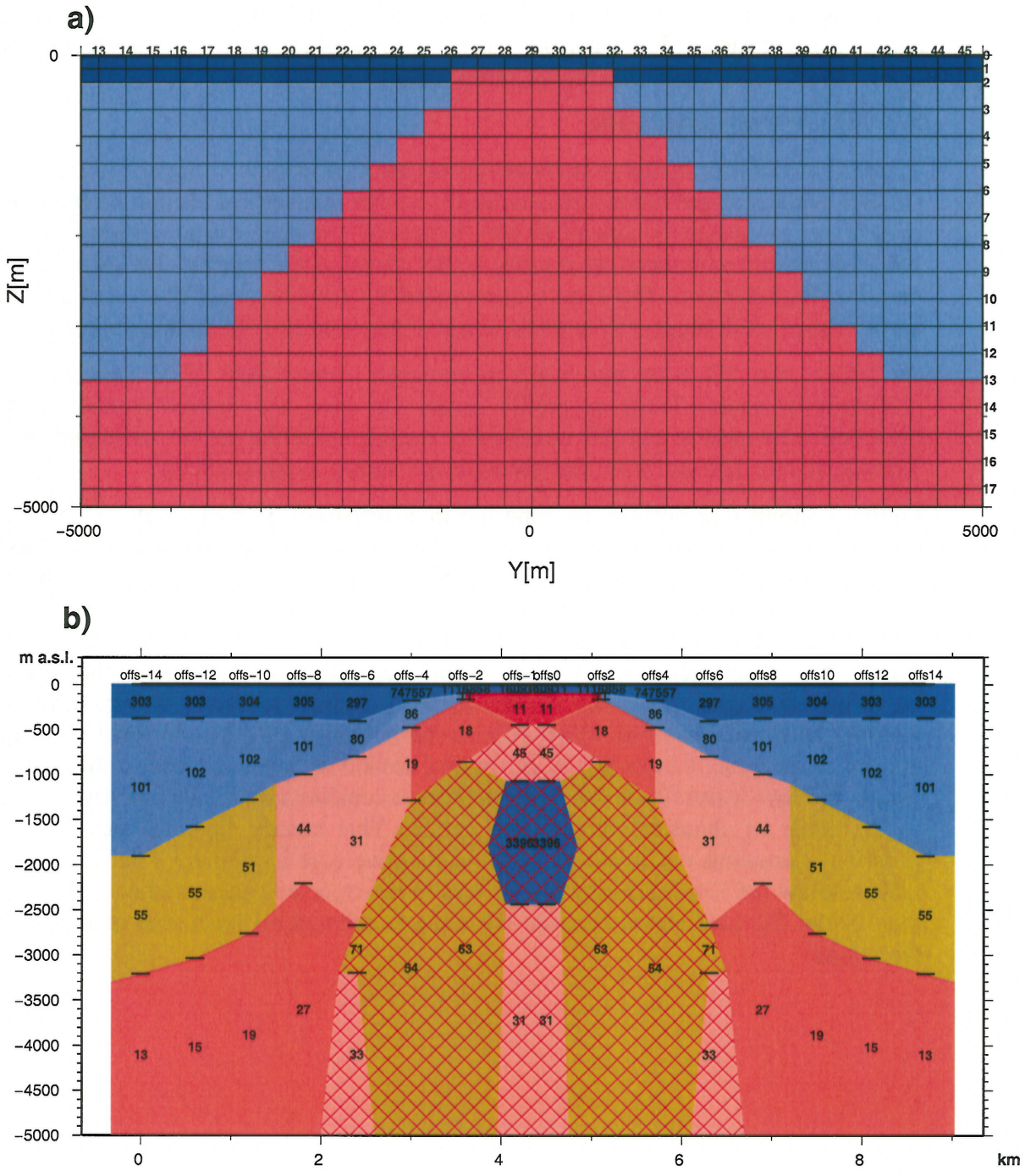

Figure-4. a), 3D 10 Ωm cone (red), dipping 45° bordered by 100 Ωm (blue), and a 1000 Ωm surface layer (dark blue). b) a resistivity section across the cone, based on 1D-inversion of synthetic central-loop sounding data.

5.4 3D conductive cone with resistive core

The final model considered here is a low-resistivity cone with a more resistive inner core, resembling the "standard model" of the resistivity structure of non saline high-temperature geothermal systems in the basaltic rocks. The model is shown in a vertical section on figure 8. It has a conical low-resistivity cap of 10 Ωm (light red) sloping by 45° down to 3.6 km depth. the thickness of the cone is about 600 m on the sides and 150 m on the top which has the diameter of 1.8 km. Inside the cone is a core of 50 Ωm (light blue). The cone is in a host of 100 Ωm (middle blue) with a 1000 Ωm surface layer (dark blue).

As before, synthetic TEM data were calculated on a profile across the cone and a section of 1D models compiled on figure 9. Figure 9 shows that the shallow resistive structure to the side of the cone is well resolved. A layer with intermediate resistivity (20–60 Ωm) is observed with generally increasing thickness and higher resistivity values away from the centre of the cone. The lower boundary of this layer reflects the lower boundary of the low-resistivity cap surprisingly well, except that the layer continues to the end of the section, well outside the anomaly.

The 1D-inversion gives somewhat complicated layering close to the top of the anomaly, with thin layers of very low resistivity sandwiching a layer of about 20 Ωm. This might be, to some extent, an artifact of limited accuracy because of the coarse grid at shallow depth and high contrasts. Below the low- and intermediate resistivity layer, a very high resistivity is obtained and much higher than the true resistivity of the model (generally of the order of thousand Ωm or more) except at the ends of the section where the basement resistivity is clearly approaching the true value, away from the anomaly.

6. Summary and conclusions

The main findings of this provisional study are that even though central-loop TEM soundings are relatively downwards focused, as compared to other sounding methods, they can be strongly affected by lateral resistivity variations. A study of the spatial and temporal distribution of intrinsic sensitivity to localised perturbations in a homogeneous half-space, shows that the sensitivity is highest on a diffuse cone that extends with time outwards and downwards from the source loop, with the maxima propagating along a cone making about 30° angle with the surface.

Even though this result applies, strictly speaking, only to a homogeneous half-space, it can probably be used as a rule of thumb when estimating whether lateral effects might be expected. Bearing this wide spread sensitivity in mind, it should not come as a surprise that horizontal variations can produce spurious effects in 1D-inversion of TEM data.

A simple study of non-1D effects in 1D-inversion shows that a 2D dipping resistivity contrast leads to higher resistivity values on the low-resistivity side, but not necessarily a higher resistivity below low-resistivity, at least not for moderate resistivity contrasts. The location of the dipping contact is fairly well indicated by the interface of a layer with intermediate resistivity and a basement with slightly higher resistivity than the true value in the model.

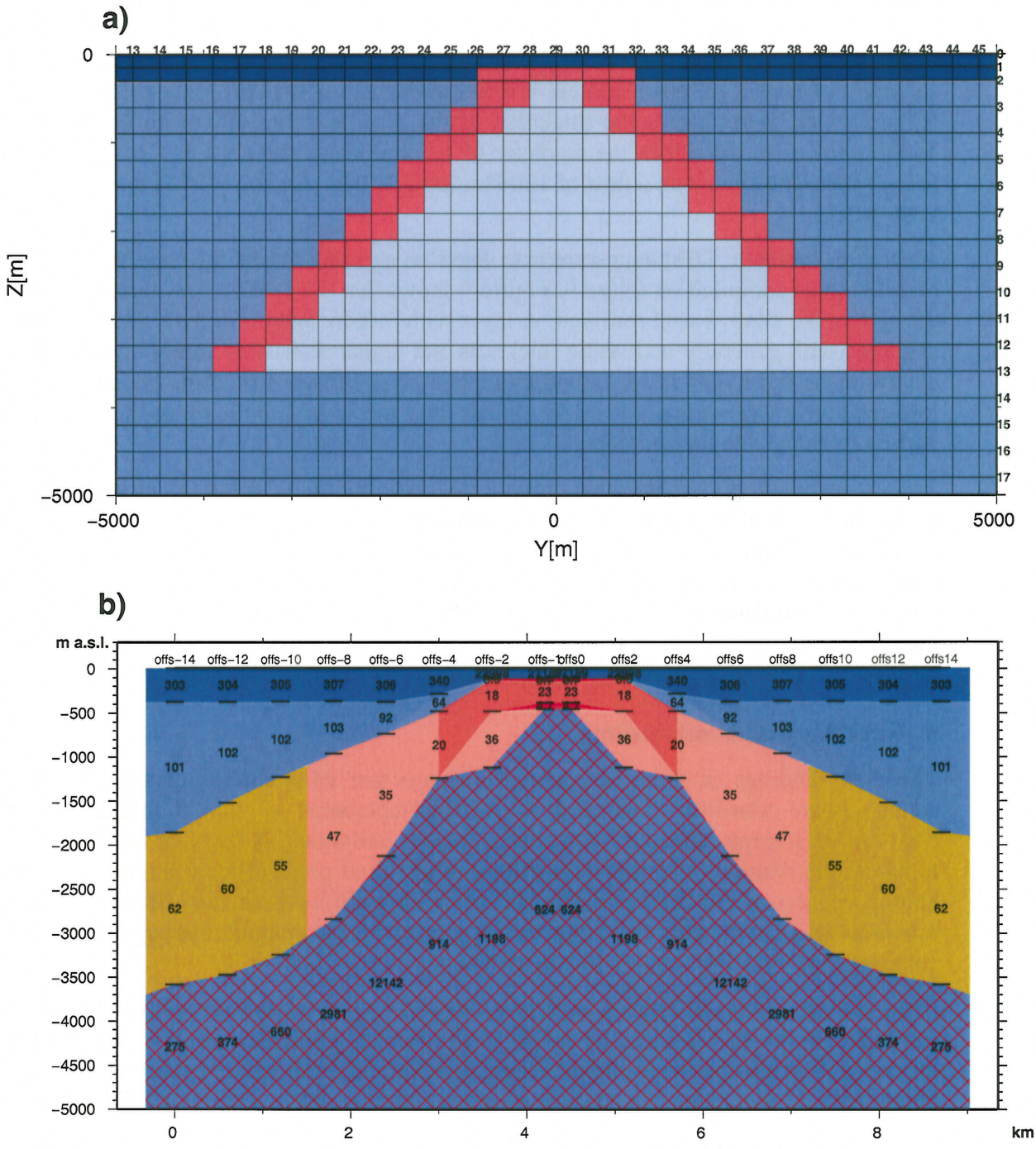

Figure-5. a), 3D 10 Ωm conical low-resistivity cap (red) with 50 Ωm inner core (light blue), bordered by 100 Ωm (blue), a 1000 Ωm surface layer (dark blue) and 50 Ωm basement. b) a resistivity section across the cone, based on 1D-inversion of synthetic central-loop sounding data.

A 2D low-resistivity ridge produces a higher resistivity under a relatively shallow low-resistivity layer under the crest and too high resistivities under the slopes of the ridge. The fictitious high resistivity values below the low-resistivity are, however, not dramatically to high, at least not for the ridge model studied here. A narrower ridge and/or higher contrast might make the effect more severe. The slopes of the ridge are, in the 1D model section, fairly well indicated by the lower boundary of a layer of intermediate resistivity, like for the dipping contact.

For a 3D conical low-resistivity anomaly surrounded by higher resistivity, the lateral variations can lead to clear, but fictitious, higher resistivity below low-resistivity in 1D-inversion. The sides of the cone are not very well resolved in the model shown here.

A 3D conical low-resistivity cap with a more resistive core gives, in 1D-inversion, much higher resistivity values in the core than in the model. The lower boundary of the low-resistivity cap seems to be fairly well mapped by the lower boundary of an intermediate resistivity layer, but this layer is, except in the vicinity of the top of the anomaly, much thicker and with much higher resistivity values than the conductive cap of the model.

It is a common feature of all the models studied here, that a 1D inversion of soundings immediately on the resistive side of dipping resistivity contrasts gives considerably lower resistivity values than the values in the models. This is of course to be expected because the soundings are influenced by the lower resistivities to the side. In all cases, a dipping layer of intermediate resistivity can be defined, with gradually increasing resistivity and thickness, away from the contact. The base of this layer seems to coincide rather well with a true resistivity contrast. It must, however, be considered highly doubtful that this be generalised to boundaries much steeper than those considered here (45°), but it is likely hold true for less steep boundaries.

The most important and practical lesson learned from the present study is that lateral resistivity variations can, under certain condition, lead to fictitious high-resistivity below low-resistivity in 1D-inversion of central-loop TEM data. This implies that care must be taken when 3D resistivity models, compiled from 1D models, are interpreted in terms of geothermal concepts. Observed higher resistivity under low-resistivity in narrow and steep anomalies can not mediately be interpreted as reflecting chlorite alteration and high temperatures.

The risk of obtaining fictitious high resistivity under low-resistivity increases with increasing steepness and contrast of resistivity boundaries. The geometries considered here, with 45° dip, are probably rather on the extreme side of what is commonly expected in real situations in geothermal areas. The hydrology of high-temperature geothermal systems and distribution of geothermal waters are, however, often largely controlled by tectonic and volcanic structures and many examples of sharp and steep boundaries are known. The example of 2D dipping contact indicates that fictitious higher resistivity is not to be expected in large resistivity anomalies because the sounding seems to have to be influenced by higher resistivity in more than one direction in order that the curve indicates higher resistivity below low-resistivity. A resistive core inside large geothermal systems seems therefor to be trustworthy, but lateral effects might produce higher values in the resistive core and at shallower depth at the edges, as is some times observed in practice.

One further important point should be made about the model with conical conductive cap and resistive core. Soundings over the slopes of the anomaly show the low-resistivity cap as a much thicker layer and with much higher resistivity than in the model, but as has been pointed out, the base of the layer fits fairly well with the lower boundary of the low-resistivity cap. It is very common, at the margins of the resistivity anomalies in high-temperature geothermal ares, where the low-resistivity cap is dipping down, to observe a conductive layer considerably thicker and with higher resistivity values than inside the main anomaly. This is strikingly similar to what is found in the model calculations.

It is sometimes practised, when presenting results of TEM surveys as iso-resistivity maps, that when a layer with intermediately low resistivity is dipping to depth and a having an under-laying high resistivity, to artificially introduce low resistivity (lower than 10Ωm) between the layer and the basement. By doing so, contour programs are forced to distinguish between the resistive inner core and high resistivity outside the geothermal system. This has been justified by saying that when going from relatively unaltered and resistive near surface rocks and down to the resistive core of the chlorite alteration, one has to go through a conductive smectite-zeolite zone. The above discussed character of the 1D inversion results for th low-resistivity cone and resistive core model strongly supports this approach.

References

Árnason, Knútur, 1984: The Effect of Finite Potential Electrode Separation on Schlumberger Soundings. 54th Annual International SEG Meeting, Atlanta, Extended abstracts, 129-132.

Árnason, Knútur, Haraldsson G.I., Johnsen G.V, Þobergsson G., Hersir G.P., Sæmiundsson K., Georgsson L.S., Rögnvaldsson S.Th, and Snorrason S.P. 1987: NESJAVELLIR-ÖLKELDUHÁLS, Surface Exploration 1986. Orkustofnun report OS-87018/JHD-02. 112pp.

Árnason, Knútur, 1995: On the effect of horizontal layering on resistivity soundings. Orkustofnun report OS-95013/JHD-08B, 12p.

Árnason, Knútur, 1999: Consistent Discretization of Electromagnetic Fields and Transient Modelling. In: Three-dimensional Electromagnetics, edit. Michael Oristaglio og Brian Spies, Geophysical developments series, v. 7, SEG. 103-118.

Árnason, Knútur, A. Kreutzmann and H. Eystinsson, 2000a: DEEP GEOTHERMAL PROSPECTING, Phase I, model calculations, Technical report. Orkustofnun report OS-2000/083, 73 pp.

Árnason, Knútur, R. Karlsdóttir, H. Eysteinsson, Ó.G. Flovenz and S.Þ. Guðlaugsson, 2000b: The Resistivity Structure of High-temperature Geothermal Systems in Iceland. Proceedings of the World Geothermal Congress WGC200, Jpan.

Day. A. and F. Morrison, 1976: Resistivity Modelling for Arbitrary Shaped Two Dimensional Structures. Lawrenc Berkeley Laboratory report, LBL-5223, UC-66a, TID-4500-R65.

Johansen, H.K., 1972: A Man/Computer Interpretation System for Resistivity Soundings

over a Horizontally Stratified Earth. Geophysical prospecting, 25, 667-691.
Nabighian, M.N., 1979: Quasi-static transient response of a conducting half-space - An approximate representation. Geophysics. Vol. 44. No. 10. 1700-1705.